

Quantum Hall spin textures far beyond the skyrmion limit

A. B. Van'kov ^{1,2}, A. S. Koreyev ¹, P. S. Berezhenoy ^{1,2} and I. V. Kukushkin^{1,2}

¹*Institute of Solid State Physics, RAS, Chernogolovka 142432, Russia*

²*Laboratory for Condensed Matter Physics, HSE University, Moscow 101000, Russia*



(Received 4 July 2022; revised 16 November 2022; accepted 13 December 2022; published 23 December 2022)

In strongly correlated quantum Hall ferromagnets with noninteger filling factors between $\nu = 1$ and $\nu = 3/2$, evidence of offbeat spin textures is obtained. The platforms for the study are two-dimensional electron systems based on MgZnO/ZnO heterostructures, in which the parameters of Zeeman and exchange energies are inconsistent with ordinary skyrmions. Experimental probing of magnetic order is fulfilled via exploration of the spectra of collective spin excitations by means of inelastic light scattering. In addition to the ferromagnetic spin exciton, a low-energy spin mode is observed, bearing witness to broken spin-rotational symmetry in the ground state. The two spin modes exhibit a pronounced anticrossing behavior, depending on the two-dimensional momentum, electron concentration, filling factor, and magnetic field tilt. The properties of the electron system are simulated using the exact diagonalization technique, showing that Landau level mixing and crossing play a key role in the nontrivial spin configuration. The corresponding spin textures emerging between $\nu = 1$ and $\nu = 3/2$ involve the orbital degree of freedom and are qualitatively different from skyrmions. Experiments at elevated temperatures show the destruction of this orbital spin texture phase with critical temperature far below the Zeeman energy. On the other side of $\nu = 1$ the textures are absent.

DOI: [10.1103/PhysRevB.106.245308](https://doi.org/10.1103/PhysRevB.106.245308)

I. INTRODUCTION

Many fundamental problems in the physics of two-dimensional electron systems (2DESs) have benefited from long-awaited progress on the experimental platform of ZnO/MgZnO heterostructures. They implement high-mobility electron systems with Wigner-Seitz parameter $r_s \sim 5\text{--}30$, which determines the dominant role of Coulomb correlations. In this previously inaccessible range of parameters 2DESs exhibit peculiar properties at extremely low temperatures and in quantizing magnetic fields. Particularly, Coulomb correlations alter the sequence of Landau levels (LLs), which causes the appearance of new phases of the integer and fractional quantum Hall effect (QHE) [1], and even an indication of Wigner crystallization at $r_s \sim 30$ has been reported [2]. Indeed, the simplest quantum Hall states with integer filling factors reveal the kaleidoscope of many-particle phenomena: Stoner ferromagnetic instability, Fermi-liquid renormalizations for electrons, and the collapse of the exchange energy [1,3–6]. The spin configuration of integer QHE states is, nevertheless, collinear and is determined by a certain composition of filled spin-up and spin-down LLs. When deviating from ferromagnetic quantum Hall states, the magnetic order becomes topologically nontrivial. Due to the competition between the exchange interaction and Zeeman coupling, skyrmion like spin textures can be realized [7,8]. The optimal size of spin texture excitations and the number of effectively flipped spins K strongly depend on the parameter equal to the ratio of the Zeeman and exchange energies, $\tilde{g} = E_z/\Sigma$. Perfect skyrmions might exist only at $\tilde{g} = 0$, but in real 2DESs, even a weak Zeeman coupling leads to a reduction in the size of spin

textures [9,10]. For example, at $\nu = 1$ and $\tilde{g} \sim 0.01$ (easily realized in GaAs-based heterostructures), the effective number of flipped spins in spin textures is $K = 3\text{--}4$, but already at $\tilde{g} \gtrsim 0.04$ textures are less beneficial than single spin flips [11]. In addition to real spin textures, numerous pseudospin textures are known in 2DESs, which involve other degrees of freedom, such as the layer index in double quantum wells and the valley index in multivalley semiconductor materials. The formation of vortexlike pseudospin textures causes the lowering of the 2DES ground state symmetry. Particularly, in tunnel-coupled double quantum wells at $\nu = 1$, the combination of spin and pseudospin degrees of freedom transforms the Heisenberg quantum Hall (QH) ferromagnet into an easy-plane Ising ferromagnet, where charged texture excitations are called merons and bimerons [12]. In various multivalley materials, including AIAs, graphene, and transition metal dichalcogenides, the interplay of the spin and valley degrees of freedom in integer QHE states leads to the appearance of numerous valley-nematic phases [13,14], as well as charged topological excitations: valley skyrmions [15].

Interaction between spin textures at filling factors deviating from $\nu = 1$ may result in noncollinear magnetic order with broken spin-rotational symmetry and supporting gapless spin-wave excitations. An analytical solution was obtained for Goldstone spin waves in a square Skyrme lattice; they have gapless linear dispersion in the long-wavelength limit [16]. The existence of the gapless spin mode dramatically alters the low-temperature physics, manifesting itself, e.g., in rapid nuclear spin relaxation [11,17]. Raman experiments [18] reveal low-energy spin waves on both sides of $\nu = 1$ under conditions favorable for the Skyrme crystal (parameter

$\tilde{g} \sim 0.013$). Low-energy spin modes are not limited to the case of the Skyrme lattice and may emerge in other noncollinear magnetic phases near $\nu = 1$ and $\nu = 3$ and at much larger values of $\tilde{g} \sim 0.15\text{--}0.3$, when skyrmions are no longer present [19]. In this case, the appearance of an extra spin wave in Raman spectra at symmetric deviations from odd filling factors again signals the breaking of the rotational symmetry in the noncollinear Hall ferromagnet, but the new mode is not truly a Goldstone boson since its energy remains finite at $k = 0$ and it couples to the Larmor mode. There is still no answer regarding whether the revealed properties of low-energy spin modes indicate a distorted microscopic structure of small-radius textures, deviations from the theoretical model used to evaluate Goldstone spin modes [16], or the absence of a long-range magnetic order. However, one thing is clear: low-energy spin modes can serve as a semaphore for the emergence of noncollinear magnetic order even in unpredictable circumstances.

One of the nonobvious cases is quantum Hall ferromagnets in ZnO-based 2DESs. In view of the fact that at $r_s \gg 1$ and at $\nu = 1$ the exchange energy of electrons is strongly suppressed [6], $\Sigma \sim \hbar \frac{eB}{m_{\text{FL}}^* c}$, with m_{FL}^* being an effective mass of Fermi-liquid quasiparticles. So exchange energy Σ , cyclotron energy $\hbar\omega_c$ ($m_{\text{ZnO}}^* \sim 0.3m_0$), and Zeeman energy $g^* \mu_B B$ ($g_{\text{ZnO}}^* = 1.95$) all turn out to be comparable. The regime of parameter \tilde{g} is thus $E_z/\Sigma \sim 1$. On the other hand, there is a renormalization of the splittings between neighboring LLs, and near their crossing, the orbital index of the levels can act as a pseudospin.

In the present work, the existence of nonskyrmion spin textures was discovered in ZnO-based 2DESs at filling factors in the range $1 \lesssim \nu \lesssim 1.5$ in conditions when the skyrmion formation was disabled due to the large Zeeman gap and the strongly reduced exchange energy. In this regime the extra spin mode, indicating broken spin-rotational symmetry in the 2D system, was found in the spectra of inelastic (or Raman) light scattering. This collective spin mode has an energy below the Zeeman scale and couples repulsively with a Larmor spin exciton at $\nu \sim 1.2$. Their energy splitting grows almost linearly as a function of the electron density and the 2D momentum, which proves the Coulomb character of the interaction. Thermal destruction of spin textures leads to the collapse of the splitting. It is shown that LL crossing at $1 < \nu < 1.5$ causes a smooth transformation of the ground state with noncollinear magnetization. The suppression of the paramagnetic phase in the whole range of filling factors by tilting the magnetic field leads to a sharp disappearance of the spin texture features. Finally, exact diagonalization studies of the energy spectrum and spin configuration confirm the role of the orbital degree of freedom in the formation of spin textures at $\nu > 1$ and their absence at $\nu < 1$.

II. EXPERIMENTAL TECHNIQUE

Experimental studies were performed on four $\text{Mg}_x\text{Zn}_{1-x}\text{O}/\text{ZnO}$ heterostructures grown by molecular beam epitaxy. A 2DES was formed in the ZnO layer near the heterointerface, occupying one size-quantized subband. Electron densities in the samples ranged from $n_s = 1.75 \times 10^{11}$ to $3.6 \times 10^{11} \text{ cm}^{-2}$ and were determined by the *in situ* method of magnetophotoluminescence. Transport mobilities in all

2DES samples exceeded $420 \times 10^3 \text{ cm}^2/\text{Vs}$. The experiment was carried out in a ^3He vapor evacuation cryostat with bath temperature $T = 0.35 \text{ K}$ in magnetic fields up to 15 T. To change the orientation of the sample with respect to the direction of magnetic field, it was placed on a rotating stage. Nonzero tilt of the magnetic field was required, first of all, to obey the selection rules for Raman scattering on spin excitons in wurtzite materials. In addition, tilting was used to control the ratio between the Zeeman and cyclotron splittings and allowed us to induce the ferromagnetic phase transition at $\nu \leq 2$. Optical measurements were performed using a tunable Ti:sapphire laser, doubled in frequency, with a wavelength in the range 366–367 nm near the direct optical ZnO gap. The magnetic field evolution of the photoluminescence signal from 2D electrons was studied to determine Landau quantization conditions, corresponding to integer filling factors. The dispersion of collective excitations was measured using the method of resonant inelastic light scattering with a tunable transferred momentum. To transmit the laser light to the electron system and to collect the scattered light signal, two quartz multimode optical fibers were used, oriented at different angles to the sample surface. Optical heating of the 2DES was excluded while using laser power densities below $5 \times 10^{-4} \text{ W cm}^{-2}$ and exploring its effect on the narrowest spectral peaks. The tilt angles of the magnetic field direction and quartz fibers were controlled separately, using the rotational stage shown in Fig. 1(a). The transferred momentum was set by the difference between the projections of the incident and scattered photons on the 2DES plane and reached values in the range of 0.4×10^5 to $3.0 \times 10^5 \text{ cm}^{-1}$. The error in transferred momenta was defined by the angles of the light cones emanating from the fibers. The signal was recorded using a spectrometer with a resolution of 1.5 \AA/mm and a liquid-nitrogen-cooled CCD camera. Statistical averaging of data from $N \sim 20\text{--}30$ raw spectra was utilized to achieve maximum accuracy in measuring the spectral positions of Raman peaks. The final error in determining the energies of collective excitations reached 3–4 μeV .

III. EXPERIMENTAL RESULTS

There are three starting points to analyze the behavior of spin excitons (SEs) in quantum Hall ferromagnets: (1) SEs exist in any locally ferromagnetic phase of the 2DES; (2) At zero momentum this excitation has a pure Zeeman energy (Larmor's theorem); (3) For the trivial case of a quantum Hall ferromagnet with $\nu = 1$, there is exactly one spin exciton branch, and its dispersion is quadratic with spin stiffness known analytically [6,20] both for small values of r_s and in the opposite limit, $r_s \gg 1$.

Figure 1(b) shows the sequence of Raman spectra focused on spin collective excitations in the sample with concentration $n_s = 2.23 \times 10^{11} \text{ cm}^{-2}$ and 2D momentum $2.12 \times 10^5 \text{ cm}^{-1}$ at different filling factors. As expected, at $\nu = 1$ there exists a single SE line with an energy shift exceeding E_z by some exchange contribution, according to its dispersion. The deviation towards $\nu < 1$ has little effect on the intensity of the line and just tunes its position. It is important that the SE line remains alone at least up to remote filling factors $\nu \sim 0.75$.

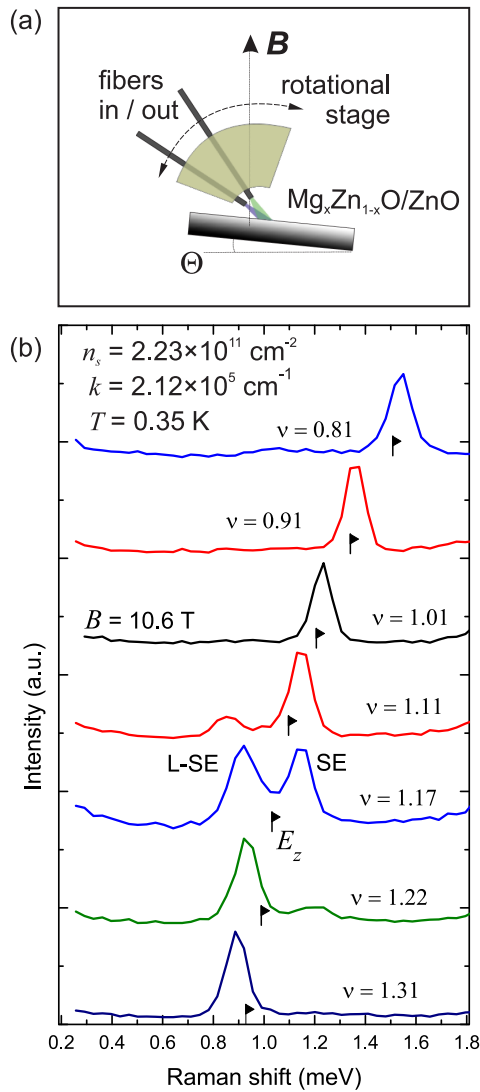


FIG. 1. (a) The schematic picture of the rotational stage, used for the Raman experiment in a tilted magnetic field with variable transferred momentum. (b) The cascade of Raman spectra of the spin exciton (SE) and low-energy spin exciton (L-SE) at different filling factors as the magnetic field is varied. The parameters of the electron density and the 2D momentum are indicated. Flags mark the positions of the Zeeman energy.

This behavior is consistent with conclusions in [21] about the conservation of the spin polarization at $\nu < 1$ in strongly correlated 2DES. The complete absence of spin textures in quantum Hall ferromagnet in ZnO under our conditions would not be surprising and would fit into the single-particle picture if they did not appear at $\nu > 1$! We clearly observe anti-crossing of the SE with another low-energy spin excitation (L-SE) mode in the range of filling factors $\nu = 1.1-1.3$. The corresponding spectra in Fig. 1(b) show an interplay of the peak intensities depending on ν . Figure 2 shows the evolution of the SE and L-SE energies as a function of the filling factor for two of the samples with different electron densities n_s and recorded at different k momenta. For convenience, the many-particle contribution to the energy is given: the trivial Zeeman term is omitted. The graph shows an asymmetric pattern of

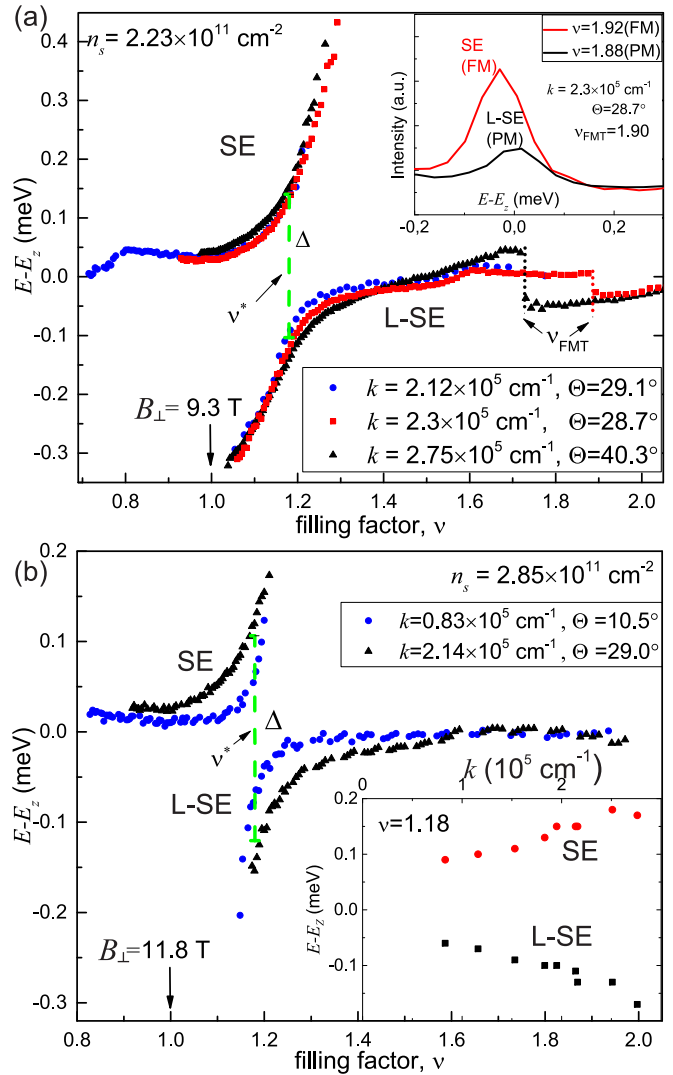


FIG. 2. Plots of many-particle contributions to the SE and L-SE energies as a function of the filling factor for two samples. (a) $n_s = 2.23 \times 10^{11} \text{ cm}^{-2}$. The values of the 2D momenta are indicated on the panels. The minimal mode splitting Δ is shown by vertical dashed lines. ν_{FMT} indicate the filling factors for abrupt ferromagnetic transition for actual tilt angles. The corresponding Raman spectra in the vicinity of ν_{FMT} are shown in the inset. (b) $n_s = 2.85 \times 10^{11} \text{ cm}^{-2}$. The inset shows the dispersions of the two spin modes at the fixed filling factor $\nu = 1.18$.

spin excitations and the presence of the L-SE mode with an energy substantially below the Zeeman splitting. The upper SE mode acquires an additional many-particle contribution to the energy at $\nu > 1$. It is noteworthy that the minimal energy splitting between SE and L-SE, their equal spectral weight, and simply their anticrossing point are found at $\nu \approx 1.18 \pm 0.01$ for all the studied samples, at small tilt angles.

By analogy with Raman studies of excitations in non-collinear quantum Hall ferromagnet in GaAs [18,19], the appearance of the L-SE is attributed to the broken spin-rotational symmetry in the ground state. We clearly see, like in [19], that the two modes coexist, couple with each other, and, consequently, emanate from the same areas with non-

collinear magnetic order. The finite energy splitting between modes can serve as an indicator of the influence of the frozen magnetic pattern on excitations. Additionally, many-particle contributions to the energy of collective excitations must also feel the 2D electron density and a transferred momentum. The inset in Fig. 2(b) shows that the repulsive energy term in the anticrossing point grows with 2D momentum. Accordingly, at $k \rightarrow 0$ the two modes arrive at E_z , which shows that the L-SE is not a true Goldstone boson and feels both the frozen magnetization in the XY plane and the Zeeman field. While approaching $\nu = 1$, the L-SE disappears, indicating that a true collinear quantum Hall ferromagnet does not support any additional spin excitons.

The observed pattern of spin modes, emerging at a one-sided deviation from $\nu = 1$, differs qualitatively from the corresponding picture in GaAs structures with the parameter $\tilde{g} \sim 0.013$ in the skyrmion limit and even outside it at $\tilde{g} \sim 0.15$. In those Raman experiments, the behavior of the two spin modes was mirrorlike at the deviation $|\nu - 1| \sim 0.1-0.3$ and reflected the skyrmion-antiskyrmion symmetry.

Two obvious parameters revealing the many-particle interaction of the modes are the electron density n_s and the wave vector k . Thus, data akin to those in Fig. 2 were obtained, and the minimal energy splitting Δ was extracted for all the samples and in the widest possible range of momenta. Figures 3(a)–3(d) depict four k dependences for the splitting at $\nu \approx 1.18$. Despite some scatter of points, a common trend is traced, a close-to-linear dependence $\Delta(k)$, and the slope increases with the electron density. In addition, the slope values were extracted from graphs using the least squares method and are plotted as a function of the electron density in Fig. 3(e). This dependence is also linear and reveals the effect of the repulsion on the many-particle interaction strength. The established dependences of the mode splitting prove the Coulomb nature of the effect. They are also in qualitative agreement with the results for GaAs-based systems [19].

The further evolution of the L-SE mode depends on the magnetic ordering of $\nu = 2$. At small tilt angles the ground state gradually transforms to a classic paramagnetic ordering, with a vanishing spin exciton at the bare Zeeman energy. At tilts exceeding $\Theta_{\nu=2} \approx 22.5^\circ$ the ferromagnetic transition occurs starting from $\nu = 2$ and crawling down to $\nu < 2$. Within the narrow transient magnetic field range $\delta B \sim 0.1$ T the system is divided into domains of the two phases, which is manifested, e.g., in the well-known resistance spikes [22]. Accordingly, the L-SE mode in a paramagnetic phase at ν_{FMT} disappears, and a ferromagnetic spin exciton emerges instead [see Fig. 2(a)]. Each phase supports just a single SE mode, and there are no signs of anticrossing and 2D spin textures around ν_{FMT} . The SE in the ferromagnetic phase at $\nu > \nu_{\text{FMT}}$ has energy below E_Z and principally different structure, as reported earlier in [23].

The transformation of the magnetic order in the range $1 < \nu < 3/2$ is qualitatively different. There the system gradually evolves from ferromagnetic to nearly paramagnetic ordering as the filling factor increases. The coexistence of the two interacting SE branches displays the nontrivial magnetic order with broken in-plane symmetry. And the evolution of these two branches depending on the B -tilt parameter is the key

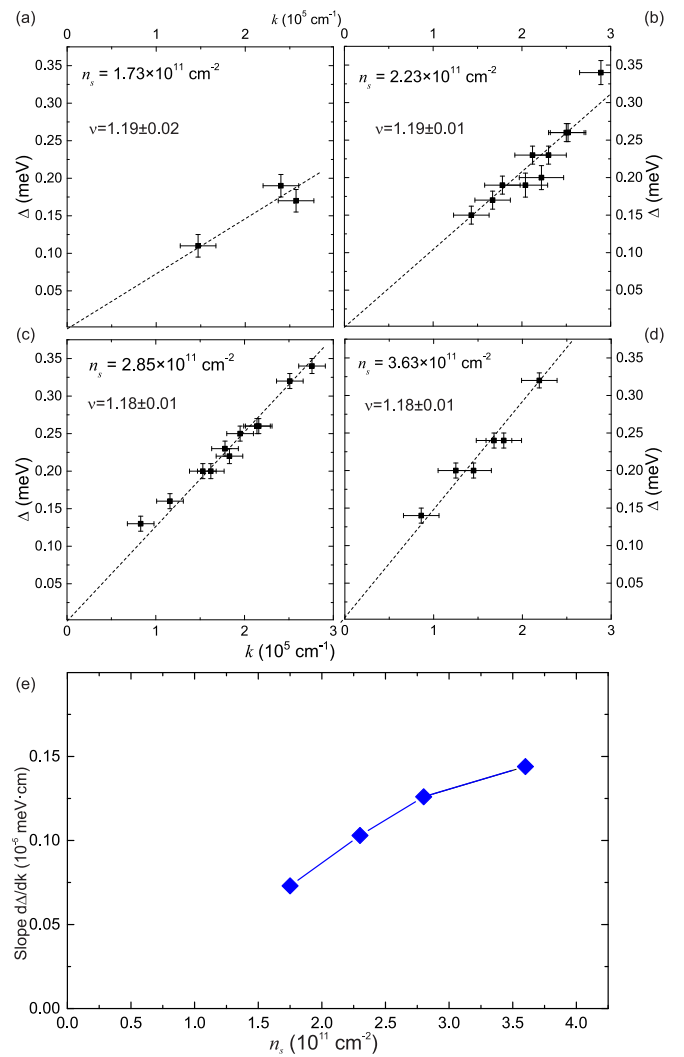


FIG. 3. (a)–(d) Dependences of the minimal splitting Δ between SE and L-SE on the wave vector k for four samples. (e) Dependence of the LMS-extracted slope from data in (a)–(d) on the electron density.

to unraveling the reasons for the emergence of a nontrivial magnetic order.

To clarify this issue, the splitting Δ was studied as a function of Θ for the sample with $n_s = 2.23 \times 10^{11} \text{ cm}^{-2}$. The graph in Fig. 4(b) represents data for the splitting between SE and L-SE over a wide range of magnetic field tilt angles Θ . In order to eliminate the linear dependence of Δ on momentum, which also changes with sample rotation, we introduced the ratio Δ/k as a measure of the influence of spin textures on the spin modes. It turns out that, up to a certain critical angle, the splitting between SE and L-SE remains at a constant level corresponding to Fig. 3(e), and then the splitting sharply drops by at least an order of magnitude (squares). The effect can be clearly seen in the spectra [Fig. 4(a)] taken in a narrow critical range of Θ and at the central filling factors ν^* . Simultaneous with a sharp drop in splitting, some shift of the central filling factor from $\nu^* = 1.18$ to about $\nu^* = 1.25$ is observed [shown by triangles in Fig. 4(b)]. The value of the critical angle at the half height of the curve breakdown

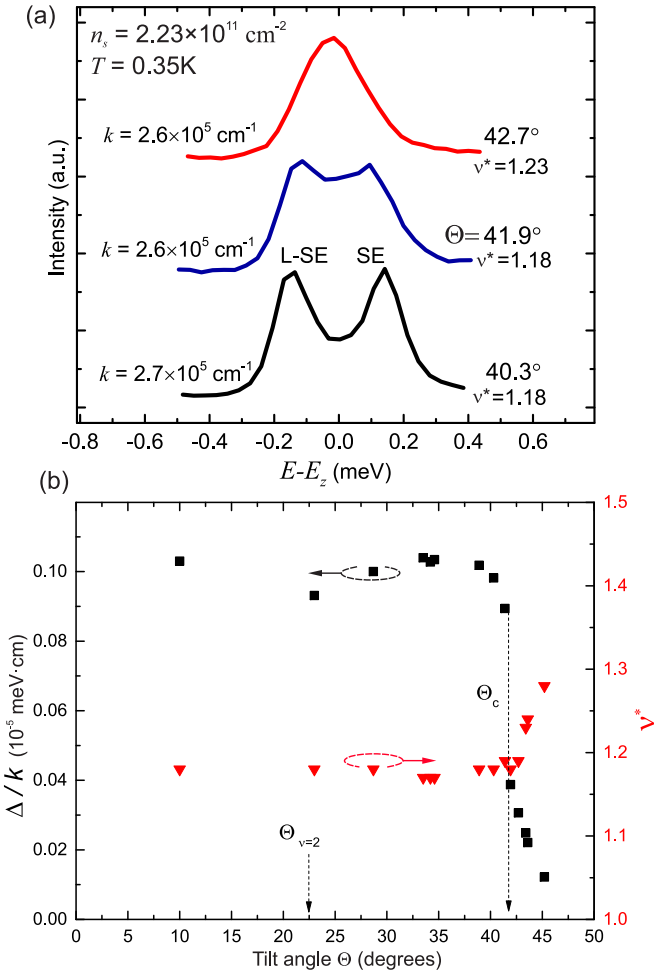


FIG. 4. (a) The set of Raman spectra of the spin modes at tilt angles close to the critical value Θ_c . (b) Spin mode splitting expressed as Δ/k as a function of the magnetic field tilt angle (squares). Triangles show the position of the central filling factor for anticrossing (right scale). The vertical arrows mark the positions of the critical tilt angles for the ferromagnetic instability at $\nu = 2$, as well as the position of Θ_c for the disappearance of spin textures.

is $\Theta_c \approx 41.7^\circ \pm 0.3^\circ$. This value is much higher than the critical angle of the ferromagnetic transition at $\nu = 2$ for this electron density [3]: $\Theta^{\nu=2FM} \approx 22.5^\circ$. Thus, to suppress the paramagnetic phase over the entire range $\nu < 2$, a much larger Zeeman splitting is required. That is why spin textures are observed even in the sample with the lowest concentration, $n_s = 1.73 \times 10^{11} \text{ cm}^{-2}$, where the $\nu = 2$ state is ferromagnetic already at small tilt angles [3]. Since the splitting between the two SE modes is attributed to a noncollinear magnetic order, it is important to find out how this order survives at increased temperatures. The thermal evolution of the modes was studied in the sample with the density, $n_s = 2.85 \times 10^{11} \text{ cm}^{-2}$, with fixed parameters k and Θ . Figure 5(a) shows a representative sequence of spectra recorded at a central filling factor ν^* . It can be seen that the splitting between the peaks noticeably decreases with temperature, and their positions approach the Zeeman energy. Figure 5(b) shows the processed dependence $\Delta(T)$ (squares) and also the integrated intensity of both peaks (diamonds). At $T \geq 3 \text{ K}$, when the peaks no longer satisfy

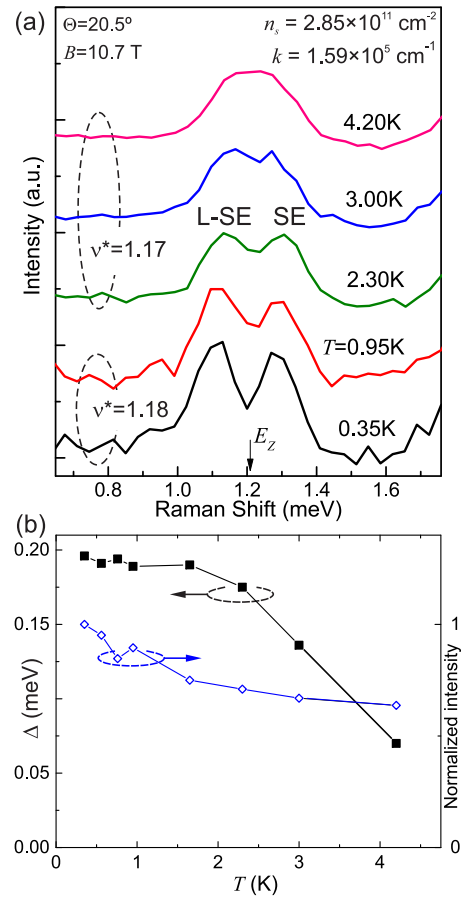


FIG. 5. (a) The cascade of Raman spectra of the L-SE and SE modes with increasing the temperature (marked on the right). The temperature dependence for the spin-mode splitting (black squares) and the integral intensity of the two peaks (diamonds).

the Rayleigh criterion, extrapolation of the positions of the one-sided lines for L-SE (at $\nu > \nu^*$) and SE (at $\nu < \nu^*$) to the point $\nu = \nu^*$ was used to refine the Δ value. In the actual temperature range, the intensity of the Raman peaks also slightly decreases due to the drop in the 2DES mobility in the MgZnO/ZnO heterostructures. Thus, at temperatures above a certain threshold, the effect of spin textures on the spin-mode splitting begins to weaken. This indicates the destruction or melting of the noncollinear magnetic order in the system.

IV. NUMERICAL SIMULATION OF THE SPIN CONFIGURATION

The properties of the quantum Hall states are determined by the key energy scales: the cyclotron, Zeeman, and many-particle Coulomb energies. At $r_s \gg 1$, a dramatic renormalization of the ferromagnetic exchange energy Σ occurs; it becomes of the order of the cyclotron energy $\hbar\omega_c^*$ with a linear rather than square-root dependence on the magnetic field. Thus, all three energy parameters are comparable, and the competition between spin and orbital transformations of the ground state is opaque. The analytical description of the problem is obstructed by the lack of a small perturbing

parameter. It is thus expedient to implement a method of exact diagonalization for a mesoscopic system of electrons.

The energy spectrum was evaluated for the states with rational filling factors on both sides of $\nu = 1$: $\nu = 8/7, 6/5, 4/3, 6/7$, and $4/5$. Unlike standard simulation schemes for fractional QHE states, in our problem it was necessary to take into account the finite LL mixing and, most importantly, to include the spin degree of freedom. For this, a basis of many-electron states at three spin-split Landau levels was used. An ensemble of N_e electrons per N_s magnetic flux quanta was considered in the torus geometry with rectangular periodic boundary conditions. The LL mixing in the calculations arose explicitly according to the scale of the Coulomb interaction at $r_s > 1$. The basis dimension of many-particle states grows superexponentially with the number of particles, so the maximum affordable parameters are about $N_s = 12$ – 15 [as indicated in Figs. 6(b)–6(d)]. The additional cutoff of the basis was introduced, taking into account the finiteness of the parameter r_s and the unfeasibility of some many-electron combinations. The influence of LLs with $n \geq 3$ was implemented by introducing a screening factor $\epsilon_s(q)$ into the Coulomb potential: the static screening method [5,24]. In this approach, the correlations between electrons at $r_s \gg 1$ are taken into account, strictly speaking, at a qualitative level. The magnetic Brillouin zone for many-particle states at noninteger filling factors had insufficient points to calculate the k dispersions of collective excitations. Therefore, the main emphasis in the calculations was placed on the energy competition between the ground states with different spin projections in order to establish which configuration is realized.

Hamilton matrices corresponding to spin projections from $S_z = -1/2N_e$ [ferromagnetic (FM)] to $S_z = (\nu/2 - 1)N_s$ [partially paramagnetic (PM)] were calculated and diagonalized. A single-particle level-filling scheme is shown in Fig. 6(a) for the two limiting cases. The competition of states with different spin projections depends primarily on the interaction strength; therefore, it is expedient to analyze the evolution of the calculated energies depending on the electron concentration or, equally, the r_s parameter. In Figs. 6(b)–6(d), the energies of various spin configurations are plotted as functions of the 2DES concentration. For the convenience of analysis, all the energies are counted from the level of the “partially paramagnetic” configuration $S_z = (\nu/2 - 1)N_s$. Naturally, the spin configuration with the lowest energy is realized in the ground state.

The main finding of the calculations is that, at large r_s values, a ferromagnetic configuration at $\nu = 1+$ is energetically more favorable than the partially paramagnetic state since curves with FM configurations are lowest in energy [open circles in Figs. 6(b)–6(d)]. Consequently, level $1 \downarrow$ is being filled by electrons instead of $0 \uparrow$ [Fig. 6(a), left]. At small r_s and increased filling factors the “partially paramagnetic” configuration is beneficial [solid squares on the right side of Figs. 6(c) and 6(d)], which corresponds to the filling of LL state $0 \uparrow$. At the intermediate parameters r_s and ν the system *gradually* evolves from ferromagnetic to paramagnetic (PM) ordering, passing through the ground states with successively flipped spins [each intersection of the curves in Figs. 6(b)–6(d)]. This smooth transformation of the magnetic order is qualitatively different from the abrupt FM-PM transition near

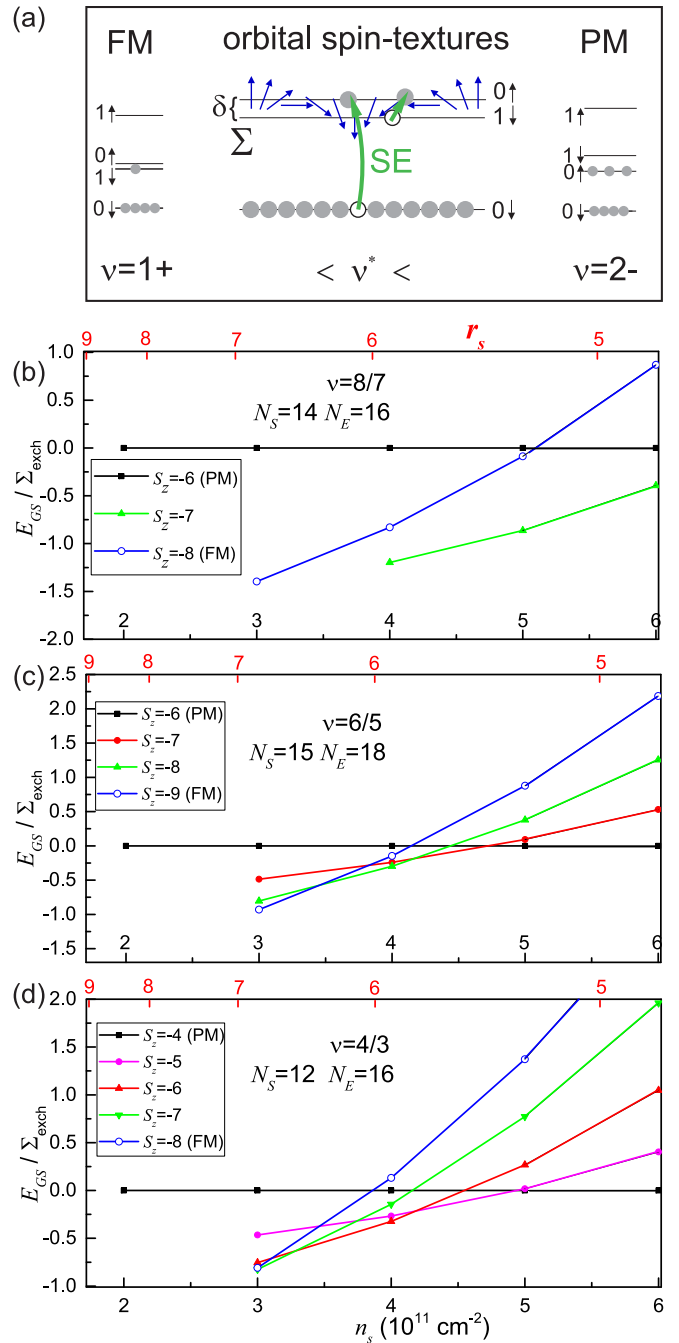


FIG. 6. (a) The occupation of quasiparticle LLs is schematically shown in inverted order ($\nu = 1+$) and direct order ($\nu = 2-$). The intermediate sketch illustrates the formation of orbital spin textures in the case when the splitting δ between $0 \uparrow$ and $1 \downarrow$ is small compared to the exchange energy Σ . Thick arrows schematically show the magnetoexciton transitions from filled to empty states, which are responsible for the formation of the two SEs. (b)–(d) The evolution of the energy of different spin configurations as a function of the 2DES concentration and the r_s parameter for three different filling factors at $\nu > 1$.

$\nu = 2$, the numerical model for which is presented in [25] and which sharply reconstructs the spin excitons [Fig. 2(a)].

Similar calculations performed for filling factors $\nu = 4/5$ and $6/7$ on the other side of $\nu = 1$ show that in the same range

of r_s , the ground state of 2DESs is ferromagnetic at the zeroth Landau level. How the anomalous filling of spin LLs at $\nu > 1$ can lead to the appearance of spin textures and noncollinear magnetic order will be explained below.

V. DISCUSSION

All previous studies of spin textures in GaAs were carried out in a regime where the exchange energy was much smaller than the cyclotron gap, and Landau level mixing was either irrelevant or was considered a weak perturbation and, rather, played against skyrmions [26]. The spin texture phases emerged symmetrically on both sides of ferromagnetic states, which is consonant with skyrmion-antiskyrmion symmetry.

In the present case, it is necessary first of all to understand what kinds of spin textures can be discussed when the Zeeman, cyclotron, and exchange energies are commensurate. The microscopic redistribution of electrons among the levels can be quite complicated at $r_s \gg 1$; instead, it is more comprehensible to consider the evolution of the ground state in terms of Fermi-liquid quasiparticles, residing on LLs with renormalized splittings. The conditions for the intersection of quasiparticle spin levels strongly depend on the filling factor. As can be seen from the data for one of the samples in this experiment [Fig. 2(a)], a sharp ferromagnetic transition occurs at reduced filling factors $\nu_{\text{FMT}} < 2$ as the magnetic field slope exceeds $\Theta_{\nu=2} \approx 22.5^\circ$. This means that at $\nu = 2$ the Landau levels are already crossed, but in a certain range of filling factors $\nu < \nu_{\text{FMT}}$, the spin configuration of the system is partially paramagnetic, corresponding to a normal hierarchy of quasiparticle LLs [Fig. 6(a), right]. The above numerical calculations show that the ferromagnetic configuration is favorable also for $\nu = 1+$, and quasiparticles prefer to occupy the level $1 \downarrow$ [see Fig. 6(a), left].

In much greater detail, the intersection of quasiparticle spin levels in the range $1 < \nu < 2$ in one of the ZnO structures with a similar density of $n_s = 2.3 \times 10^{11} \text{ cm}^{-2}$ has been studied using the magnetotransport method [27]. The magnetoresistance map recorded at $T = 400 \text{ mK}$ shows a strongly nonmonotonic ν dependence of the magnetic field tilt angle required to cross the $0 \uparrow$ and $1 \downarrow$ levels. The maximum angle ($\approx 41.8^\circ$) is required for $\nu \approx 3/2$. Moreover, from the side with $\nu > 3/2$, the contrast of the magnetoresistance and, accordingly, the ferromagnetic transition looks sharp, and in the region where $1 < \nu < 3/2$, at all tilt angles up to the maximum, a transition region strongly smeared in terms of the filling factor is observed. Significant growth of the critical tilt angle at noninteger filling factors $\nu < 2$ is apparently due to the much greater screening of the Coulomb interaction. Hence, the Fermi-liquid renormalization of the splittings is less pronounced, and the largest tilts are required for crossing at $\nu \approx 3/2$. Thus, the magnetotransport data also indicate that the intersection of quasiparticle spin levels at $1 < \nu < 3/2$ is fundamentally different from the avalanchelike ferromagnetic transition at $\nu \approx 2$. The only textures possible for that case are one-dimensional domain walls between the two phases and are described using a simple Ising model [28].

In the current situation, the calculations of the ground state for $1 < \nu < 3/2$ show precisely the successive character of spin flips with variations in both the electron density and the

filling factor, where the role of electron-electron correlations is dominant. It is obvious that the calculations for a small number of electrons are not sufficient to demonstrate a smooth spin rotation; only discrete switchings to more favorable spin configurations are visible. In terms of quasiparticle levels, this may mean that their intersection does not occur abruptly, and in a certain extended range of filling factors, levels $0 \uparrow$ and $1 \downarrow$ nearly coincide. This is where that the parameter of vanishingly small energy splitting δ emerges, being much less than the exchange energy on Landau levels Σ . By analogy with the skyrmion story, at a change in the filling factor, the transfer of quasiparticles between the two close spin levels occurs through the formation of smooth spin textures. Since the orbital degree of freedom is involved, they can be called *orbital spin textures* [see Fig. 6(a), middle]. And although the parameters of the intersecting levels are unknown, we can assume that growth in δ affects the decrease in the texture size, and further filling of the $0 \uparrow$ level at $\nu \rightarrow 3/2$ will continue according to the single-particle scenario. It should be emphasized that this mechanism for the appearance of spin textures immediately fails as soon as the paramagnetic phase completely disappears at filling factors $1 < \nu < 2$, for example, at large tilts of the magnetic field.

The key difference in the behavior of the magnetic order in such a model from the skyrmion scenario is its one-sided character. As is known, ordinary skyrmions and antiskyrmions on opposite sides of $\nu = 1$ lead to equally fast transfers of electrons from the lower to the upper spin states of the zeroth Landau level, equalization of their population, and complete spin depolarization. In the actual case, the quasiparticles do not just transfer between levels $0 \uparrow$ and $1 \downarrow$ in the form of spin textures; the energy levels themselves eventually swap. As a result, the entire collective of quasiparticles passes from the upper to the lower of these two levels with a gentle change in the exchange energy, and this transition is unidirectional.

The type of magnetic ordering and the size of the orbital spin textures are unknown since they depend on the ratio of the effective spin gap δ to the exchange energy Σ , which is not available. Nevertheless, it can be argued that the textures are two-dimensional since they support the two coupled spin modes in the bulk. To minimize the total exchange energy, the spin alignment in the adjacent textures must be matched by analogy with a Skyrme lattice, but it is impossible to assert the presence of a long-range order without theoretical clues. The nonzero gap of the L-SE at $k = 0$ is rather in favor of a short-range spin texture fluid, like in Ref. [19].

The formation of two interacting spin modes in the orbital spin texture phase can be schematically represented as two kinds of magnetoexcitons between quasiparticle levels $0 \downarrow \rightarrow 0 \uparrow$ and $1 \downarrow \rightarrow 0 \uparrow$ [see Fig. 6(a), middle]. If there are quasiparticles at each of the levels $0 \downarrow$ and $1 \downarrow$, then both transitions are possible. Each magnetoexciton has a Zeeman contribution with the same sign, so interaction between them is permitted by symmetry. At $\nu > 1$ and at a certain distribution of quasiparticles over levels $0 \uparrow$ and $1 \downarrow$, both magnetoexcitons exist and interact with each other and with the frozen magnetization pattern. The latter mechanism of coupling may strongly depend on the spin texture pattern and is absent for an ideal Skyrme lattice. In our case it is unknown but resembles the character of the spin mode mixing reported

for the short-range spin texture liquid [19]. When the $1 \downarrow$ level is emptied, only the $0 \downarrow \rightarrow 0 \uparrow$ transition remains.

The linear increase in the energy splitting between the two spin modes as a function of the electron concentration fully corresponds to the nature of the growth of the renormalized exchange energy at $r_s \gg 1$. In addition to the purely exchange contribution, this quantity also includes the energy of the direct dipole-dipole interaction, from which it is also natural to expect renormalization from the square-root scale $e^2/\epsilon\ell_B$ to the linear $\hbar\omega_c$, which was shown experimentally and theoretically [5,29,30]. The linear in momentum energy contributions can arise for two reasons: the first is due to the presence of a magnetization gradient of spin textures, and second, in the anticrossing regime, the two spin excitons have a dipole-dipole repulsion with an off-diagonal Coulomb matrix element proportional to $M_{1,2} \sim k$. The latter was established, for example, in the theoretical consideration [23,31] of spin excitations in the $\nu = 2$ ferromagnetic phase.

The observed temperature behavior of the spin modes means the destruction of the noncollinear magnetic order, that is, the smearing of the spin inhomogeneities in the XY plane. The same scenario is expected for both liquid and crystalline spin texture phases, which cannot be distinguished by our method. A qualitatively similar behavior of the soft spin mode was observed in GaAs heterostructures [18] when the energy deviation from E_z collapsed with elevated temperature and showed the melting of the supposedly Skyrme lattice phase. The data obtained here for one sample are not enough to establish the origin of the critical temperature, but it can be said for sure that this temperature is much lower than the scale of the Zeeman energy, which is $T_z \approx 14$ K for the conditions of Fig. 5. In this sense, the spin texture phase is more fragile than the quantum Hall ferromagnet $\nu = 1$, with T_z being a critical temperature.

Surprisingly, Θ_c coincided with the critical angle 41.8° when the $\nu = 3/2$ incompressible QHE state forms in ZnO samples with close electron densities [27]. Thus, the disappearance of orbital spin textures and the alignment of electron spins at the two lowest LLs are crucial for the emergence of

new exotic fractional states with half-integer filling factors involving an orbital degree of freedom. Additional study at low temperatures is desirable to determine the role of incompressible fractional QHE states in the evolution of magnetic order at $1 < \nu < 3/2$, as well as the origin of the central filling factor $\nu^* \approx 1.18$, which seems to be invariant.

VI. CONCLUSION

In strongly correlated 2DESs based on MgZnO/ZnO heterostructures evidence of a broken symmetry ground state with noncollinear magnetic order was obtained at filling factors between $\nu = 1$ and $\nu = 3/2$. Experimental probing of the magnetic order was fulfilled by means of inelastic light scattering on collective spin excitations. Apart from the ordinary Larmor spin exciton a spin mode with energy below the Zeeman gap was discovered, which indicates a broken spin-rotational symmetry in the XY plane. The two spin modes couple at filling factors around $\nu^* \approx 1.18$ via Coulomb interaction, as their splitting grows monotonically with the electron density and the 2D momentum. In the studied systems the Zeeman, cyclotron, and exchange energy scales are comparable; hence, ordinary skyrmions are not possible. It was shown that noncollinear magnetic order can be due to spin textures of the orbital type, emerging at the intersection of renormalized quasiparticle Landau levels $0 \uparrow$ and $1 \downarrow$, which was confirmed by the exact diagonalization studies at $1 < \nu < 3/2$. Experiments with tilted magnetic fields showed that orbital spin textures disappear as soon as the paramagnetic phase disappears between $\nu = 1$ and $\nu = 2$. Heating of the 2DES to temperatures $T \sim 2$ K leads to the thermal destruction of the orbital spin texture phase.

ACKNOWLEDGMENTS

The authors are grateful to the Russian Science Foundation (Grant No. 22-12-00257) for their support for performing experiments on Raman scattering and RFBR (Grant No. 20-02-00343) for support for performing the calculations.

-
- [1] J. Falson and M. Kawasaki, *Rep. Prog. Phys.* **81**, 056501 (2018).
 - [2] J. Falson, I. Sodemann, B. Skinner, D. Tabrea, Y. Kozuka, A. Tsukazaki, M. Kawasaki, K. von Klitzing, and J. H. Smet, *Nat. Mater.* **21**, 311 (2022).
 - [3] A. B. Van'kov, B. D. Kaysin, and I. V. Kukushkin, *Phys. Rev. B* **96**, 235401 (2017).
 - [4] V. V. Solov'yev and I. V. Kukushkin, *Phys. Rev. B* **96**, 115131 (2017).
 - [5] A. B. Van'kov, B. D. Kaysin, S. Volosheniuk, and I. V. Kukushkin, *Phys. Rev. B* **100**, 041407(R) (2019).
 - [6] A. B. Van'kov and I. V. Kukushkin, *Phys. Rev. B* **102**, 235424 (2020).
 - [7] H. A. Fertig, L. Brey, R. Cote, and A. H. MacDonald, *Phys. Rev. B* **50**, 11018 (1994).
 - [8] L. Brey, H. A. Fertig, R. Cote, and A. H. MacDonald, *Phys. Rev. Lett.* **75**, 2562 (1995).
 - [9] A. H. MacDonald, H. A. Fertig, and L. Brey, *Phys. Rev. Lett.* **76**, 2153 (1996).
 - [10] H. A. Fertig, L. Brey, R. Cote, A. H. MacDonald, A. Karlhede, and S. L. Sondhi, *Phys. Rev. B* **55**, 10671 (1997).
 - [11] S. Melinte, E. Grivei, V. Bayot, and M. Shayegan, *Phys. Rev. Lett.* **82**, 2764 (1999).
 - [12] L. Brey, H. A. Fertig, R. Cote, and A. H. MacDonald, *Phys. Rev. B* **54**, 16888 (1996).
 - [13] M. Kharitonov, *Phys. Rev. B* **85**, 155439 (2012).
 - [14] S. A. Parameswaran and B. E. Feldman, *J. Phys.: Condens. Matter* **31**, 273001 (2019).
 - [15] Y. P. Shkolnikov, S. Misra, N. C. Bishop, E. P. De Poortere, and M. Shayegan, *Phys. Rev. Lett.* **95**, 066809 (2005).
 - [16] R. Côté, A. H. MacDonald, L. Brey, H. A. Fertig, S. M. Girvin, and H. T. C. Stoof, *Phys. Rev. Lett.* **78**, 4825 (1997).
 - [17] S. E. Barrett, G. Dabbagh, L. N. Pfeiffer, K. W. West, and R. Tycko, *Phys. Rev. Lett.* **74**, 5112 (1995).

- [18] Y. Gallais, J. Yan, A. Pinczuk, L. N. Pfeiffer, and K. W. West, *Phys. Rev. Lett.* **100**, 086806 (2008).
- [19] I. K. Drozdov, L. V. Kulik, A. S. Zhuravlev, V. E. Kirpichev, I. V. Kukushkin, S. Schmult, and W. Dietsche, *Phys. Rev. Lett.* **104**, 136804 (2010).
- [20] Yu. A. Bychkov, S. V. Iordanskii, and G. M. Eliashberg, *JETP Lett.* **33**, 143 (1981).
- [21] A. B. Van'kov, B. D. Kaysin, and I. V. Kukushkin, *JETP Lett.* **110**, 268 (2019).
- [22] E. P. De Poortere, E. Tutuc, S. J. Papadakis, and M. Shayegan, *Science* **290**, 1546 (2000).
- [23] A. B. Van'kov and I. V. Kukushkin, *Phys. Rev. B* **104**, 165144 (2021).
- [24] W. Luo and T. Chakraborty, *Phys. Rev. B* **93**, 161103(R) (2016).
- [25] A. B. Van'kov, B. D. Kaysin, and I. V. Kukushkin, *Phys. Rev. B* **98**, 121412(R) (2018).
- [26] V. Melik-Alaverdian, N. E. Bonesteel, and G. Ortiz, *Phys. Rev. B* **60**, R8501 (1999); I. Mihalek and H. A. Fertig, *ibid.* **62**, 13573 (2000).
- [27] J. Falson, D. Maryenko, B. Friess, D. Zhang, Y. Kozuka, A. Tsukazaki, J. H. Smet, and M. Kawasaki, *Nat. Phys.* **11**, 347 (2015).
- [28] T. Jungwirth and A. H. MacDonald, *Phys. Rev. Lett.* **87**, 216801 (2001).
- [29] S. Dickmann, *Phys. Rev. B* **65**, 195310 (2002).
- [30] S. V. Iordanski and A. Kashuba, *JETP Lett.* **75**, 419 (2002).
- [31] S. Dickmann and B. D. Kaysin, *Phys. Rev. B* **101**, 235317 (2020).